

Variable-Length Genetic Algorithm and Multiple Entropic Functions-Based Satellite Image Segmentation



Ramen Pal, Somnath Mukhopadhyay, and Debasish Chakraborty

Abstract The genetic algorithm (GA) was invented to mimic the realistic biological evaluation for optimization. But, in literature, we can observe that the genetic operators are purely based on either mathematical or random operations. Our proposed genetic operators are designed to mimic realistic behavior. For this purpose, we have introduced the concept of gene casements in crossover and Levy flight function in mutation. We have also incorporated solution combination operation to give it an elitist nature. Otsu's, Tsallis, and Reyni's entropic functions were validated as efficient thresholding techniques. Researchers weren't able to conclude which method is superior among them. Their performance is highly dependent on the dataset. So, we have considered all of these methods to frame our methodology. We have considered the dataset from the WorldView-2 satellite sensor for the experimental study. The performance of the proposed method is validated with three different state-of-the-art methods.

Keywords VHR image · LULC segmentation · Variable-length GA · Lèvy flight · Entropic function

1 Introduction

Multi-spectral image segmentation is the procedure of distinguishing different objects or land-use land-cover (LULC) classes in a satellite image. The success of remote sensing applications like, LULC change detection [1], prediction [2], identification [1], etc., solely depend on the efficiency of the backhand segmentation algorithm [3]. In literature, we can observe that satellite image segmentation algorithms are framed by using: (i) edge, (ii) region, (iii) cluster, (iv) artificial neural network,

R. Pal · S. Mukhopadhyay (✉)

Department of Computer Science and Engineering, Assam University, Silchar, India

e-mail: som.cse@live.com

D. Chakraborty

RRSC-East, ISRO, Kolkata, India

© The Author(s), under exclusive license to Springer Nature Singapore Pte Ltd. 2023
S. Basu et al. (eds.), *Proceedings of International Conference on Frontiers in Computing and Systems*, Lecture Notes in Networks and Systems 404,
https://doi.org/10.1007/978-981-19-0105-8_22

223

(v) thresholding, etc. [4–9]. Among these approaches, cluster- and threshold-based segmentation techniques are proven as efficient [10, 11]. Clustering is a method to separate a satellite image into distinct classes. All the elements within a class should be highly cohesive, and between the classes are highly coupled in nature [12]. Clustering-based techniques generally suffer with problems like, (1) stacking into the regional optima, (2) highly dependent on initialization. These issues can be solved by using metaheuristic-based techniques. It can produce high-quality segmented images. Metaheuristic algorithms like, genetic algorithm, particle swarm optimization, ant colony optimization, cuckoo search, and multi-objective optimization(MOO) algorithms are useful for these purposes. Whereas, thresholding techniques find out optimal ranges with respect to color information. A range is defined as a LULC class. This is done by using the help of entropic functions. In last few decades, entropic functions like, Tsallis, Otsu's, Kapur, Rènyi, etc., are extensively used to segment an image with bi-modal or multi-modal histogram. These functions did not have any optimization tool to optimize these threshold values. This issue can be resolved by hybridizing a metaheuristic algorithm with entropic function. In literature, all the previous researches in this regard are suffering with issues like: (i) automatic identification of the total number distinct LULC classes within a satellite image and (ii) identification of proper entropic function as objective. Justification of the efficiency of an entropic function will not be proper. Since the performance of a function depends on the types of the satellite image. It is proven that Tsallis, Otsu's, and Rènyi's entropic functions are efficient in two different aspect like, types of the image and modal of the histogram. But, researchers weren't able to conclude that a particular entropic function is highly efficient compare to others in general. So, we should formulate the objective function of an optimization method by considering these aforementioned functions. In a satellite image, total number of LULC classes varies with the image. So, there is a strong need to create a variable-length nature for an algorithm that can cope-up with this situation. Genetic algorithm (GA) is one of the prominent metaheuristic approaches that solve optimization problems efficiently. But, this algorithm suffers with the following issues: (i) In mutation, this algorithm states that some weakest genes should be updated to make the chromosome more efficient. This should be done with respect to the fittest solution. But, in reality, some random changes are applied. (ii) Elitism is optional, and (iii) In crossover, dissimilar portion of both of the parent chromosomes should be considered. But, in reality, similar portions of gene sequences are also considered. So, it motivated us to propose an image segmentation method that is free from all of these dependencies or issues. Contributions of this paper are as follows:

1. A new approach toward designing a variable length and elitist satellite image thresholding algorithm.
2. Considering Tsallis, Otsu's, and Rènyi's entropic function collectively to formulate the objective function.
3. Automatic identification of the total number distinct LULC classes within a satellite image.

4. Proposing a new realistic technique for mutation by using Leÿy flight generation function.
5. Proposing a new realistic technique for crossover by using gene casements.

In the rest of the paper, Sect. 2 considered the discussion on the proposed methodology, Result and analysis are presented in Sect. 3, and conclusion is presented in Sect. 4.

2 Proposed Methodology

It is a two-step process. In the first step, threshold values for the satellite image are optimized, and corresponding segmentation is done. Then, in the second step, classes obtained in the segmented images are mapped with the proper LULC class by using ground truthing information. The proposed algorithm is presented in 1.

First, initial encoding of c number of chromosomes are done. Here, a chromosome is represented as a vector. It represents a combination of b number of solutions. Here, b represents the total number of bands in an input image. Each solution represents a probable set of threshold values for a band of the input image. All solutions will have equal length (l). Value for l is chosen randomly. Here, b represents the total number of bands in an image. Since the input image can have bi-modal or multi-modal histogram. So, we have limited the value for l . It should be ≥ 2 . By iterating the above-mentioned procedure, we have encoded c number of chromosomes. After that, genetic operators and corresponding operations are applied iteratively based on a condition. In this process, first, the fitness value (F) of each chromosome is evaluated by using Eq. 1. Here, O_E represents the average Otsu's Entropy for i th chromosome.

$$F_i = \left(\frac{\sum_{i=0}^b O_E}{b} + \frac{\sum_{i=0}^b T_E}{b} + \frac{\sum_{i=0}^b R_E}{b} \right) / 3 \quad (1)$$

It is a non-parametric and between class variance function. It maximizes the inter-cluster distance. It is presented in Eq. 2.

$$O_E = \sum_{i=0}^m \sigma_i \quad (2)$$

Here, m represents the total number of threshold values. σ_i represents the between class variance of the i th class. It is calculated by using Eq. 3.

$$\sigma_i = \omega_i \times (\mu_T - \mu_i)^2 \quad \text{Where, } 0 \leq i \leq n \quad (3)$$

Here, ω represents the summation of probability of intensity values. μ_T represents the global mean of intensity values, and μ_i represents the mean intensity value for i th

Algorithm 1: Variable-length and Elitist Genetic Algorithm Based Satellite Image Segmentation and Change Detection Method.

Input: MS imagery (*img*), Number of iterations (*z*), Size of the population(*c*)
Output: Segmented or Thresholded Image
Begin;
b= Total number of bands in the input image;
Initial population is randomly encoded with *c* number of chromosomes. Here, the length of each gene is *b* ; // $2 \leq \text{chromosome length} \leq 20$
for *g* = 1 to *z* **do**
 if *g* = 1 **then**
 Fitness of each chromosome is evaluated by using Equation 1;
 Store the fittest chromosome in G_{best} ;
 Roulette wheel or fitness proportionate selection is done to select the mating pool *m* of size *c*;
 Real coded crossover function is applied on *m*;
 Real coded mutation function is applied on *m* by using G_{best} ;
 end
 else
 Combined mating pools of current and previous generations to create a pool with $2 \times c$ number of chromosomes;
 Fitness of each chromosome is evaluated by using Equation 1;
 Select the fittest chromosome (*P*);
 if *P* is fittest than from G_{best} **then**
 | $G_{best} = P$.
 end
 Roulette wheel or fitness proportionate selection is done to select the mating pool *m* of size *c*;
 Real coded crossover function is applied on *m*;
 Real coded mutation function is applied on *m* by using G_{best} ;
 end
end
Combine current and previous mating pools to constitute a combined pool;
From the combined pool, the fittest chromosome (*S*) is selected as the optimal sets of threshold values for image segmentation;
Calculate the global threshold values by taking mean of *b* number of solutions within *S*;
Number of clusters (*K*)= length of *S*;
K number of clusters by using the optimal threshold values for each cluster from *S*;
Classify each class in the segmented image to a LULC class by using ground truth information;
End;

class. Here, O_E is a maximization function. T_E is the Tsallis entropy measure. It is an elicitation of Boltzman–Gibbs entropy measure. It is a measure to a non-extensive system. It is presented in Eq.4.

$$T_E = \sum_{i=0}^m S_q^i(t) \quad (4)$$

Here, q is the Tsallis parameter. t represents the threshold value, and S^i represents the Tsallis entropy. It is represented in Eq. 5.

$$S_i = \frac{1 - \sum_{i=1}^t P_i^q}{q - 1} \quad (5)$$

It is a multi-fractal theory-based formula. Here, P_i represents the probability of the system and is in state i . Here, T_E is also a maximization function. R_E is the R nyi's entropy measure. It is an elicitation of Shannon entropy. It is presented in Eq. 6.

$$R_E = \sum_{i=0}^m R_\alpha(A_i) \quad \text{Where, } \alpha > 0 \quad (6)$$

Here, α is a non-substantial control parameter. The value for α should be greater than 0. A_i is the elicitation of the Shanon entropy. It is calculated by using Eq. 7.

$$R_\alpha = \frac{1}{1 - \alpha} \ln \sum_{i=1}^L P_i^\alpha \quad \text{Where, } \alpha > 0 \quad (7)$$

Here, P_i represents the probability distribution of the i th class. L defines the total number of threshold. R_E is also a maximization function. Fitness value for a chromosome is calculated by taking the mean of O_E , T_E and R_E . After that, for the first iteration, fitness proportionate selection is done only to select c number of solutions from the population to create a mating pool of size c . It is evident that the convergence rate of this selection strategy is higher than others. The chance of selection of a chromosome is proportionate to its fitness value. In the rest of the iteration, a combined mating pool is generated before selection. This combined pool is generated by combining all solutions from the previous generation with the solutions from the current generation. This operation ensures elitism. Then, reproduction is done by using genetic operator. In biological evaluation, crossover doesn't produce child chromosomes that are drastically different from the parent one. In literature, existing crossover methods doesn't consider this behavior. We have designed our algorithm in such a way that it exhibits the realistic behavior. In this method, two chromosomes (P_1 and P_2) are randomly selected first. Then, a probabilistic value C_j is randomly chosen. If this value is less than the thresholded crossover probability (C_p), then crossover is applied. In a crossover operation, first, the common gene casements (gc) between P_1 and P_2 are extracted. If the length of gc is greater than 1, then the minimum value between total number of gene casements (m_{P_1} and m_{P_2}) of chromosome P_1 and P_2 is selected. Then, first, m number of gene casements are swapped between P_1 and P_2 . Else, one among two different operations are executed based on a probabilistic value (act). If this value is greater than 0.5, then 0.5 is subtracted from all genes that are presented in gene casements of P_1 and P_2 . Otherwise, 0.5 is added. This operation ensures the the avoidance of premature convergence. This process is repeated for $n/2$ times. Then, the length of each solution in a chromosome is restricted. For

example, the input image has three bands. So, the chromosome is comprised with three solutions. Each solution represents a probable threshold values for a band. Let, the solution with minimum number of gene is P_S . Since our algorithm has variable-length behavior with respect to chromosomes and the chromosomes are represented as vector. All solutions within a chromosome should have equal length. So, the length of each solution is restricted with the length of P_S . After that, mutation is applied. In reality, a chromosome is mutated by updating its gene to make it more fit. So, we can get efficient genes if we update it with respect to the globally fittest chromosome (G_{best}). $G - \text{best}$ represents fittest chromosome among the all previous generations. In our method, a gene is mutated based on a probabilistic value (m_j). If it is less than the thresholded mutation probability (m_p), then g_i is updated by using the Lévy flight formula. Otherwise, it is updated by subtracting 0.1% value of each threshold values g_i in g . Lévy flight is an elicitation of Brownian motion. It produces short amount of (C) but random jumps toward the globally fit solution. It is presented in Eq. 8.

$$C = 0.01 \times S \times (g_i - b_g) \text{ Where, } 0 \leq i \leq b \quad (8)$$

Here, S is the random step. It is generated by using the symmetric Lévy flight distribution. g_i and b_g are current gene and global best gene, respectively. The overall process is executed for 200 iterations. After completing all the iterations, a combined mating pool is generated by combining the mating pool of current and last generation. The fittest solution (S) from this pool is selected as the optimal set of threshold values for segmentation. Then, the global threshold values are calculated by taking the mean of threshold values obtained for b number of bands. After that, the input image is segmented by using S . If the length of S is n , then we get $n + 1$ number of segments in the segmented image.

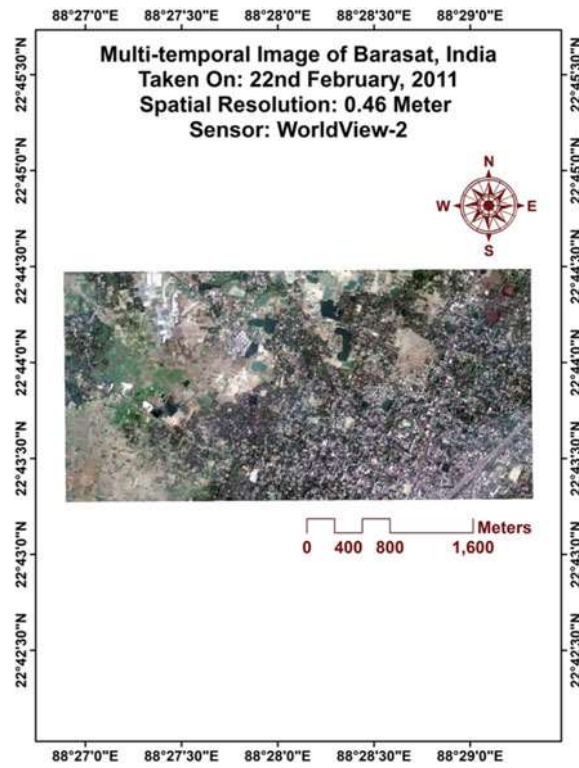
3 Results and Discussions

In this section, the effectiveness of the proposed method is analyzed and validated with respect to three different state-of-the-art methods. All the experiments on the proposed method are done on a system with Software: Python 3.7 and ArcMap-10.5, Operating System: Windows-10, CPU: Intel(R)-Core(TM)-i5, and RAM: 8 GB. Apart from that, a GPS handheld device is used to perform the ground truthing to assess the accuracy of the segmentation. All the images are represented in the form of map. These maps are created by using ArcMap-10.5 software.

3.1 Experimental Results

We have considered VHR and PAN-sharpened multi-spectral image of Barasat, India, taken from WorldView-2 satellite sensor. This dataset is taken on February 22, 2011 and has a spatial resolution 0.46 m. It has 3 bands. It is shown in Fig. 1.

Fig. 1 Experimental VHR image of Barasat, West Bengal, India, with a spatial resolution 0.46 m, obtained from WorldView-2 satellite sensor, taken on December 14, 2020



The proposed method is executed on this dataset. We considered the size of the initial population as 100 and its executed for 200 iterations. The fittest solution from the final combined pool is selected. Then, global threshold values are calculated by considering the mean of all fittest chromosomes for all bands of the input image. Then, thresholding is performed to segment the input image using it. After that, it is classified into 4 different LULC classes (waterbody, built-up, vegetation, and bare soil) based on the ground truthing information. Then, methods of Eddine et al. [13], Xing et al. [14], and Mousavirad et al. [15] are executed on the input image, and the quality of segmentation is quantified for validation. The qualitative results obtained after classification are presented in Fig. 2.

We can observe that the quality of the results obtained by our proposed method is better than other methods. We have quantitatively validated this claim in Table 1. The internal performance of all segmentation methods is validated by using Dunn index [16], Davies Bouldin (DB) index [17], and Silhouette score [18]. We can observe that our proposed method outperforms other techniques in all cases. So, we can conclude that our proposed method can segment a satellite image with a complacent performance. Finally, the accuracy of the classification is quantified by using the Kappa Co-efficient (K) [19]. In this process, 100 random locations (latitude and longitude information) from the study area are selected. Then, we visited those

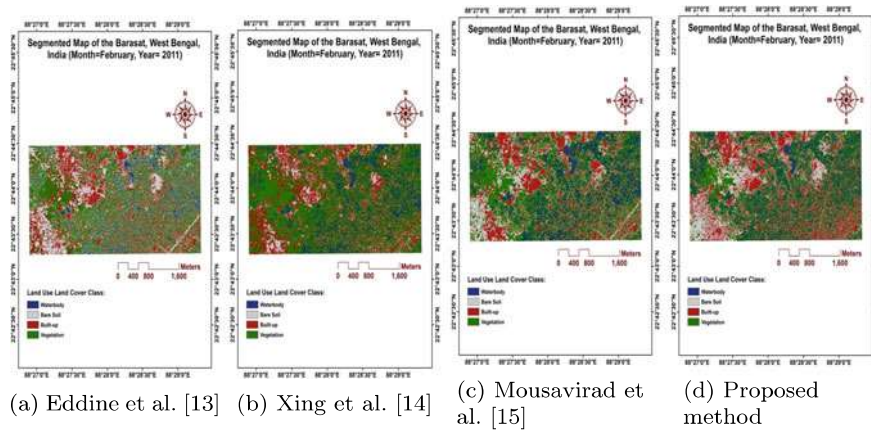


Fig. 2 Segmented images generated by the: **a** Eddine et al. [13], **b** Xing et al. [14], **c** Mousavirad et al. [15], and **d** Proposed method

Table 1 Performance validation of the proposed method

Algorithm	Dunn score	DB score	Silhouette score	Kappa co-efficient
Eddine et al. [13]	1.0914324519	0.3865482180	0.4525618565	0.8616
Xing et al. [14]	0.9971457920	0.6519437862	0.4032873154	0.8002
Mousavirad et al. [15]	1.2722518245	0.1640250640	0.5502160820	0.9000
Proposed method	1.4006205845	0.1109200425	0.5810586427	0.9275

areas; check the real LULC class. Then, actual and predicted LULC classes are stored in an excel sheet. In the Table 1, superior performance of a method regarding a metric is presented using bold characters. Then, this data is used to calculate the value for K . We can observe that our proposed has the highest K score compared to other methods. So, we can also conclude that our proposed method is fair accurate.

4 Conclusion and Future Scope

We proposed a new technique for satellite VHR image thresholding by using our proposed improved GA. We have also discussed a way of defining realistic crossover and mutation operation by using the gene casements and Lèvy flight generation function, respectively. We have also shown that Tsallis, Otsu's, and Rènyi's entropic function collectively can produce better segmentation result. Our method can optimize the total number of output clusters automatically. Our proposed method is tested by

using the dataset from WorldView-2 satellite sensor. It outperformed three different state-of-the-art methods in respect of four different evaluation parameters.

This method is based on ground truthing. So, a way of doing classification without ground truthing need to be find out in future.

References

1. Dey V, Zhang Y, Zhong M, A review on image segmentation techniques with remote sensing perspective. In: Proceedings of the international society for photogrammetry and remote sensing symposium (ISPRS10) XXXVIII (Part 7A)
2. Zhang D, Islam MM, Lu G (2012) A review on automatic image annotation techniques. *Pattern Recogn* 45(1):346–362. <https://doi.org/10.1016/j.patcog.2011.05.013>
3. Mitra P, Shankar BU, Pal SK (2004) Segmentation of multispectral remote sensing images using active support vector machines. *Pattern Recogn Lett* 25(9):1067–1074. <https://doi.org/10.1016/j.patrec.2004.03.004>
4. Satapathy S, Raja NSM, Rajinikanth V (2018) Multi-level image thresholding using otsu and chaotic bat algorithm. *Neural Comput Appl* 29:1285–1307. <https://doi.org/10.1007/s00521-016-2645-5>
5. Jain S, Laxmi V (2018) Color image segmentation techniques: a survey. In: Proceedings of the international conference on microelectronics, computing & communication systems. Springer Singapore, Singapore, pp 189–197
6. Yu H, He F, Pan Y (2018) A novel region-based active contour model via local patch similarity measure for image segmentation. *Multimedia Tools Appl* 77:24097–24119. <https://doi.org/10.1007/s11042-018-5697-y>
7. Guo Y, Şengür A, Akbulut Y, Shipley A (2018) An effective color image segmentation approach using neutrosophic adaptive mean shift clustering. *Measurement* 119:28–40. <https://doi.org/10.1016/j.measurement.2018.01.025>
8. Singh V, Misra A (2017) Detection of plant leaf diseases using image segmentation and soft computing techniques. *Inf Process Agric* 4(1):41–49. <https://doi.org/10.1016/j.inpa.2016.10.005>
9. Zhang HCM, Zhang L (2010) A neutrosophic approach to image segmentation based on watershed method. *Signal Process* 90(5):1510 – 1517, special Section on Statistical Signal and Array Processing. <https://doi.org/10.1016/j.sigpro.2009.10.021>
10. Liang Y, Zhang M, Browne WN (2014) Image segmentation: a survey of methods based on evolutionary computation. *Simulated evolution and learning*. Springer International Publishing, Cham, pp 847–859
11. Senthilkumaran N, Rajesh R (2009) Image segmentation—a survey of soft computing approaches. *International conference on advances in recent technologies in communication and computing* 2009:844–846. <https://doi.org/10.1109/ARTCom.2009.219>
12. Ruspini EH (1969) A new approach to clustering. *Inf Control* 15(1):22–32. [https://doi.org/10.1016/S0019-9958\(69\)90591-9](https://doi.org/10.1016/S0019-9958(69)90591-9)
13. Salah Eddine M, El Joumani S, Zennouhi R, Masmoudi L, Multi-objective optimization for worldview image segmentation funded on the entropies of tsallis and rényi, *Multimedia Tools and Applications* 79. <https://doi.org/10.1007/s11042-020-09572-4>.
14. Xing Z (2020) An improved emperor penguin optimization based multilevel thresholding for color image segmentation. *Knowl-Based Syst* 194:105570. <https://doi.org/10.1016/j.knosys.2020.105570>
15. Mousavirad SJ, Ebrahimpour-Komleh H (2020) Human mental search-based multilevel thresholding for image segmentation. *Appl Soft Comput* 97:105427. <https://doi.org/10.1016/j.asoc.2019.04.002>

16. Rivera-Borroto OM, Rabassa-Gutiérrez M, Grau-Ábalo R, Marrero-Ponce Y, Vega J (2012) Dunn's index for cluster tendency assessment of pharmacological data sets. *Can J Physiol Pharmacol* 90:425–33. <https://doi.org/10.1139/y2012-002>
17. Pakhira MK, Bandyopadhyay S, Maulik U (2004) Validity index for crisp and fuzzy clusters. *Pattern Recogn* 37(3):487–501. <https://doi.org/10.1016/j.patcog.2003.06.005>
18. LaHaye N, Ott J, Garay MJ, El-Askary HM, Linstead E (2019) Multi-modal object tracking and image fusion with unsupervised deep learning. *IEEE J Sel Top Appl Earth Obs Remote Sens* 12(8):3056–3066
19. Xu L, Jing W, Song H, Chen G (2019) High-resolution remote sensing image change detection combined with pixel-level and object-level. *IEEE Access* 7:78909–78918